

# Simulations and Effects of Natural Environments on Low Frequency Antennas with Three-Dimensional FDTD Method

Julien Vincent<sup>1, \*</sup>, Pierre Borderies<sup>1</sup>, Jean-René Poirier<sup>2</sup>, and Vincent Gobin<sup>1</sup>

**Abstract**—Three-dimensional Finite-Difference in Time-Domain method is applied to simulate Low Frequency antennas in the presence of natural environments. All antennas are made up of wires set down on a square shaped ground plane and their dimensions depend on the wavelength of the source. Both monopole and inverted L antennas are considered in this paper. The antenna systems are computed in the presence of two examples of natural elements: a large forest and then on the top of a hill. The main aim of this paper is to show the effects of these environments on the properties of the antennas and on the efficiency of the ground wave excitation. The outcome of these investigations shows a power ratio enhancement of several decibels when the two kinds of antenna described in this paper are located on the top of a hill. On the other hand, the effects of a large forest depend on the geometry of the antenna. It doesn't affect the radiation of a quarter-wave monopole antenna, on the contrary losses disrupt radiation when an inverted L antenna is built in the middle of a large forest.

## 1. INTRODUCTION

Low Frequency band (LF) is also known as the kilometer band because the wavelengths  $\lambda$  range from 100 m to 10 km. The radio waves can travel long distance with — at least — three propagation modes: direct (line-of-sight), surface (groundwave) and ionospheric (skywave) modes. Antennas used to transmit information at these frequencies are mainly wire type antennas [1] and the electromagnetic field propagation over usual soils is known [2, 3]. These papers and the references herein deal with the radiation of a dipole over a flat terrain, or over an irregular one at a significant distance from the dipole. As shown in [3], the problem may be split in two steps: the computation of the radiated field at approximately three wavelengths and then the subsequent computation of the propagation with propagation algorithms. For the first step, according to the type of antenna and ground several approaches may be used including full wave ones like integral equation with vertically stratified media [4], which is available in commercial codes. These full wave approaches do not consider to our best knowledge the irregularities of the terrain in the vicinity of the antenna, and however it is well known that such irregularities are influent on the radiation properties since their experimental observations are widely reported, see [5] for example. It is interesting to know how the ground wave reacts when the antenna system is located close to natural elements and how it affects its excitation. The goal of this paper is to treat their 3D modelling.

Finite-Difference in Time-Domain (FDTD) is a well-known method used for computational electromagnetics [6, 7]. The advantages of this technique include a wide frequency range with one single run simulation and conveniences to treat heterogeneous dielectric materials. This method is perfectly adequate here but on the other hand, this scheme requires an upper bound on the time-step, which depends upon space steps to ensure numerical stability and, at low frequencies, we at least have to represent the details of the antenna, leading to small mesh cells. In [8], bi-dimensional FDTD algorithm

---

*Received 7 May 2014, Accepted 10 August 2014, Scheduled 16 August 2014*

\* Corresponding author: Julien Vincent (julien.vincent@onera.fr).

<sup>1</sup> Electromagnetism and Radar Department — ONERA, 2 Avenue Edouard Belin, Toulouse 31000, France. <sup>2</sup> Research Group in Electromagnetism — LAPLACE INPT, 2 Rue Charles Camichel, Toulouse 31071, France.

is applied to calculate the field strength of Low Frequency (LF) ground wave propagating over irregular terrains. In this paper, three-dimensional FDTD is applied to compute LF wire antennas in the presence of two types of natural environments.

The paper is organized as follows. In Section 2, FDTD method and its principles are described and the formalism of wires is presented. The efficiency of the boundary conditions is then examined and discussed. The geometries of the computed antennas are chosen and all results of the numerical simulations are presented in Section 3. The positions for the antennas are in the middle of a large and high forest and on the top of a hill. In the last part, the conclusions and future prospects are presented.

## 2. PRINCIPLES OF COMPUTING AND DESIGN OF THE ANTENNAS

In our FDTD code, all wires are implemented with Holland and Simpson formalism [9]. A voltage source can be added on the wire with a time signal known as Rayleigh pulse [10] which presents a null zero-frequency component, helpful for Fourier Transform and frequency domain analysis. The soil of the Earth is considered in this paper as an infinite homogeneous half-plane with relative permittivity  $\varepsilon_{rs}$  and electrical conductivity  $\sigma_s$ . These parameters depend on the characteristics of the soil and representative values can be found in [11] and reported in Table 1.

**Table 1.** Dielectric constants and conductivities for different soils.

Earth's soils	$\varepsilon_{rs}$	$\sigma_s$ ( $\text{S} \cdot \text{m}^{-1}$ )
Dry	5	$10^{-4}$
Medium wet	15	$10^{-3}$
Wet	30	$10^{-2}$

Boundary conditions are important parameters in electromagnetic modeling with FDTD. The spatial domain of the computed field is unbounded in real life but it has to be confined for antenna modeling. An absorbing boundary condition is introduced in order to exponentially attenuate the electromagnetic field to reduce reflection. Since they were introduced by Berenger in [12], the *Perfectly Matched Layers* (PML) have been extended in many papers [13, 14]. It has been illustrated clearly in [15] that a strong numerical reflection occurs from the PML of Berenger at low frequencies. Uniaxial-PML (UPML) [16] are then used here to terminate the three-dimensional numerical domain because care should be taken in extending the soil inside the boundary layers. The PML loss parameters are determined by a geometric grading. Firstly, conductivity  $\sigma_0$  at the interface is computed with

$$\sigma_0 = -\frac{\ln(R) \cdot \ln(g)}{2Z_0\Delta_i(g^N - 1)} \quad (1)$$

where  $R$  is the reflection coefficient,  $g$  the scaling factor,  $Z_0$  the impedance of free space,  $\Delta_i$  the space step in the PML direction, and  $N$  the number of PML cells. Then the PML loss factor is given by the average value in the cell around the index location  $L$ :

$$\sigma_e(0) = \sigma_0 \cdot \frac{\sqrt{g} - 1}{\ln(g)} \quad (2)$$

$$\sigma_e(L > 0) = \sigma_e(0) \cdot g^{L-1/2} \quad (3)$$

In this paper, the PML parameters are set to  $R = 10^{-4}$ ,  $g = 2$  and  $N = 10$  in all computations. Fig. 1 shows the geometry of the problem solved by Sommerfeld [17]: an infinitesimal vertical electric dipole over a dielectric half-space ( $\varepsilon_0\varepsilon_{rs}, \mu_0, \sigma_s$ ) is computed with FDTD and UMPL boundaries. The electric current element  $I_0l$  at height  $h$  above the soil transmits to a receiver  $M$  at height  $z$ .

At  $f_0 = 100$  kHz, with  $l = 25$  m,  $h = 37.5$  m and  $z = 1$  m, propagation of vertical component  $\mathbf{E}_z$  over a medium wet soil, along the distance  $r$  is solved with two different methods: FDTD and the Method of Moments computed with the integral solver of the industrial software *FEKO*. The results, shown in Fig. 2, demonstrate the efficiency of the chosen and implemented boundary conditions and the

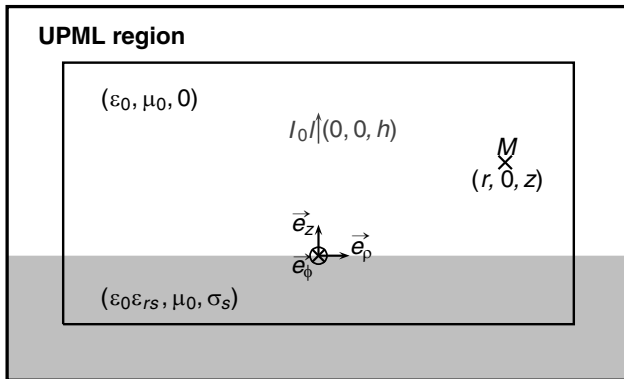


**Figure 1.** Geometry of the problem of Sommerfeld for FDTD computation. The vertical  $z$ -directed electric current element  $I_0 l$  is at height  $h$  above a planar soil with electrical parameters  $(\epsilon_0 \epsilon_{rs}, \mu_0, \sigma_s)$ . The receiving point  $M$  is at height  $z$  and distance  $r$ . UPML boundaries terminate the three-dimensional numerical domain.

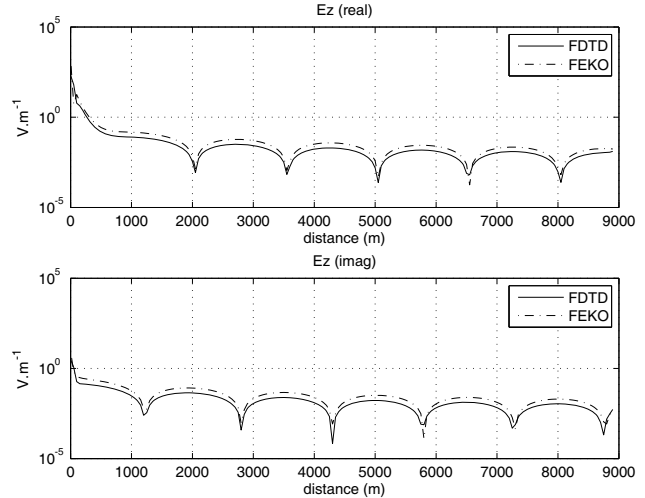


**Figure 2.** Solution comparison of the problem of Sommerfeld with two different methods, FDTD and MoM computed with the integral solver of *FEKO*. The vertical electric complex — real and imaginary parts — component  $\mathbf{E}_z$  with logarithmic scale is computed along the distance  $r$  from  $\lambda_0/10$  to  $3\lambda_0$  at  $f_0 = 100$  kHz (300 m to 9 km).

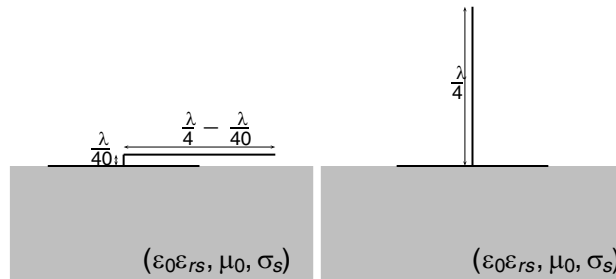


**Figure 3.** Geometry of the antennas. The inverted L antenna, a small vertical wire ( $dl = \lambda_0/40$ ) and a bigger horizontal one ( $dL = \lambda_0/4 - \lambda_0/40$ ), is on the left and the quarter-wave monopole antenna is on the right. Both antennas are in the middle of a squared ground plane (width =  $\lambda_0/4$ ).

modeling of the soil for our distance of interest: from  $\lambda_0/10$  to  $3\lambda_0$ . Remotely from this distance, one can use propagation techniques of DeMinco [3]. More complex natural environments can be implemented in the FDTD model which is done in the following.

### 3. RESULTS AND DISCUSSIONS

The simulated antennas are an inverted L antenna and a quarter-wave monopole antennas at the frequency  $f_0 = 100$  kHz. They are both made up of two parts: a wire and a square shaped ground, as shown in Fig. 3. We shall now introduce the examples of natural environments.

#### 3.1. Large Forest

According to [18], a forest can be represented by a dielectric slab with corresponding dielectric constant  $\epsilon_{rf}$  and  $\sigma_f$  for this range of frequency. The values ( $\epsilon_{rf} = 1.065; \sigma_f = 10^{-3} \text{ S} \cdot \text{m}^{-1}$ ) are used here for a 25 m high forest.

### 3.1.1. Inverted L Antenna

At the frequency  $f_0 = 100$  kHz, an inverted L antenna is located at the center of a square shaped (width = 12 km, height = 25 m) forest. Fig. 4 and Fig. 5 show the results of the simulations. On the first one the squared magnitude of the electric field  $|\mathbf{E}|^2$  is sampled at 9 km around the antenna, 1 m over the ground and then normalized by the input power. In Fig. 5 the power ratio in dB is sampled along the  $y$  direction of propagation, 1 m over the ground.

One can observe in Fig. 4 that the shape of the radiation pattern does not change when this type of antenna is placed in the forest. Nevertheless a 10 dB loss occurs with the natural element. The modelling in Fig. 5 shows that the signal partially recovers itself beyond the forest at 6 km. This effect is similar to the Millington recovery effect [19]. However due to losses inside the dielectric slab, the power density at the end of the forest is smaller than the power density obtained with the flat bare soil case.

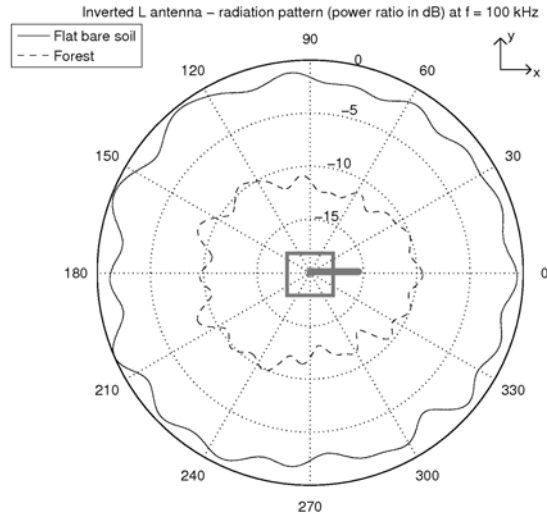


**Figure 4.** Simulations of an inverted L antenna at  $f = 100$  kHz with and without the large forest. The antenna is drawn in the middle, according to the axes orientation the horizontal wire is along  $x$  direction.

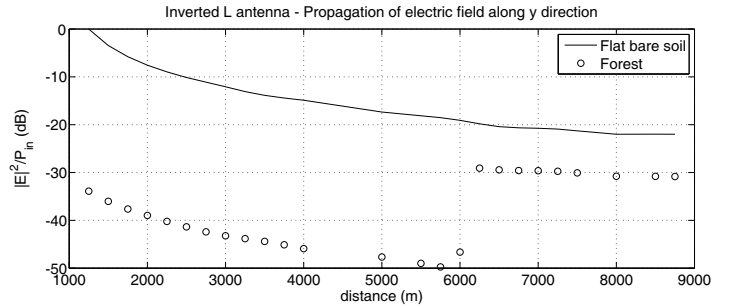


**Figure 5.** Simulations of an inverted L antenna at  $f = 100$  kHz with and without the large forest along  $y$  direction from 1.2 km to 9 km. With the environment a recovery effect known as Millington effect is observed at the end of the forest (6 km).

### 3.1.2. Quarter-Wave Monopole Antenna

The same methodology was applied to a quarter-wave monopole antenna emitting at  $f_0 = 100$  kHz. It was computed in the presence of the forest described in the previous section. The squared magnitude of the electric field  $|\mathbf{E}|^2$  at 9 km around the antenna and 1 m over the ground is normalized by the input power.

As shown in Fig. 6 the radiation patterns are similar, one deduces that the forest do not interfere with this type of antenna. This is quite logical because only a small part of the antenna is inside the forest in this (rather theoretical) case. This is confirmed with the results in Fig. 7. The power ratio is lower in the forest from 0 to 6 km and it completely recovers itself a little further.

The studies of these two antenna systems reveal that in both cases the shape of the radiation pattern is not affected by the introduction of the forest but losses appear with the inverted L antenna. At the same frequency, the difference between an inverted L antenna and a quarter-wave monopole antenna is the presence of the horizontal wire. On inverted L antennas, which is a narrowband antenna, the vertical wire is the radiating element and the horizontal one is used for impedance matching. Two effects are observed when this type of antenna is placed in a high forest. First a frequency shift occurs with the forest in the nearfield excitation because the gap between the horizontal capacitive wire and the

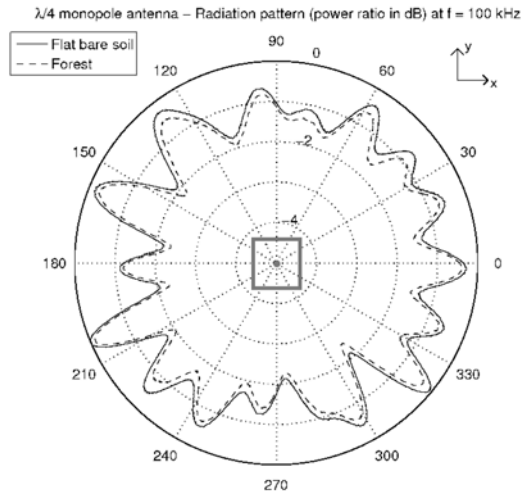


**Figure 6.** Simulations of a quarter-wave monopole antenna with and without the forest. At  $f_0 = 100$  kHz, the antenna is built in the middle of the system and the results are sampled at 9 km around it and normalized by the input power.

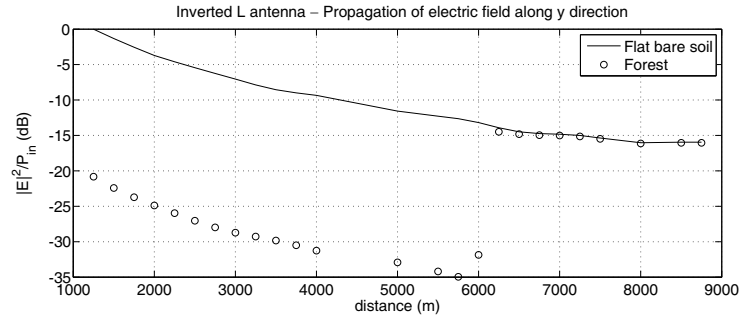


**Figure 7.** Simulations of a quarter-wave monopole antenna at  $f = 100$  kHz with and without the forest along  $y$  direction from 1.2 km to 9 km.

soil is modified by the presence of the forest. This frequency change is taken into account by the input power normalization. Secondly one can observe power losses presumably due to the natural element which absorbs a part of the energy emitted by this antenna.

### 3.2. On the Top of a Hill

The cartesian grid of the FDTD method requires the use of multiple dielectric blocks defined by  $(\epsilon_{rh}; \sigma_h)$ . They are created with different sizes in order to build a hill with an average slope, see Fig. 8. The hill and the soil have the same dielectric constants  $(\epsilon_{rh} = \epsilon_{rs}; \sigma_h = \sigma_s)$ .

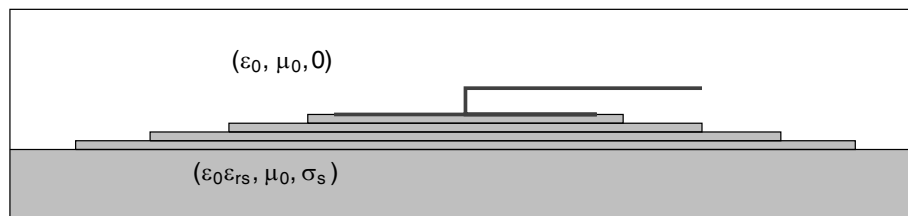


**Figure 8.** Hill created for FDTD simulations, in this case: four 25 m height dielectric slabs are stacked on each other, their widths are chosen in order to create an average eleven percent slope. The height of antennas equals three times of the height of a dielectric slab. The antenna is located on the top of the hill.

#### 3.2.1. Inverted L Antenna

An inverted L antenna at the frequency  $f_0 = 100$  kHz is located on the top of a hill made up of 4 square shaped dielectric blocks. All of them are 25 m high and their width are calculated so as to create an eleven percent average slope.

The interactions with two different soils — dry ( $\epsilon_{rs} = 5; \sigma_s = 10^{-4} \text{ S} \cdot \text{m}^{-1}$ ) and medium wet ( $\epsilon_{rs} = 15; \sigma_s = 10^{-3} \text{ S} \cdot \text{m}^{-1}$ ) — are computed here. Fig. 9 and Fig. 11 show the results of the

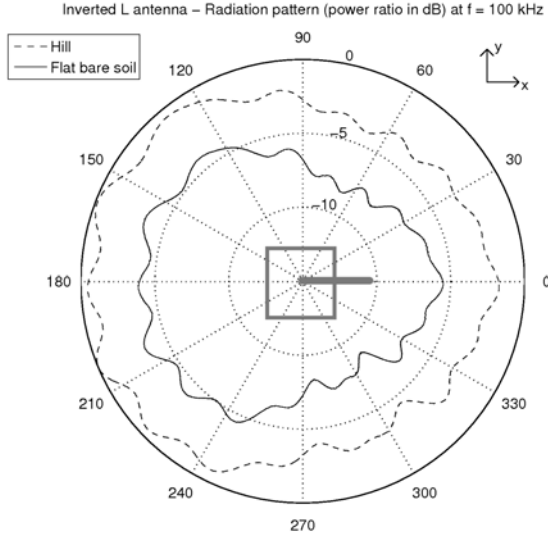


**Figure 9.** Simulations of an inverted L antenna at  $f = 100$  kHz with and without the hill on dry soil ( $\epsilon_{rs} = 5$ ;  $\sigma_s = 10^{-4} \text{ S} \cdot \text{m}^{-1}$ ). The squared magnitude of the electric field is sampled at 9 km around the antenna and 1 m over the ground and normalized by the input power.

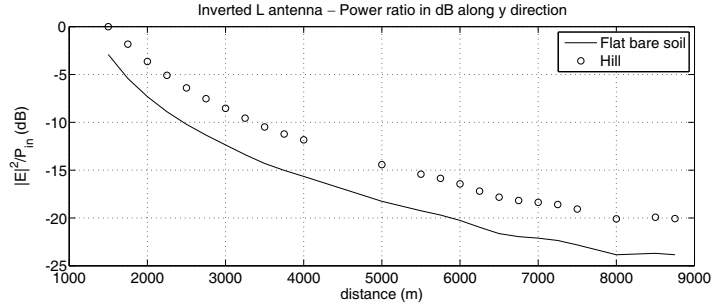


**Figure 10.** Simulations of an inverted L antenna with and without the hill on dry ( $\epsilon_{rs} = 5$ ;  $\sigma_s = 10^{-4} \text{ S} \cdot \text{m}^{-1}$ ) soil along  $y$  direction.

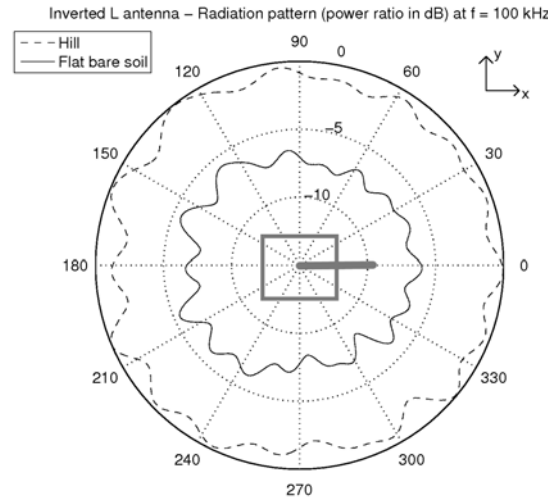


**Figure 11.** Simulations of an inverted L antenna at  $f = 100$  kHz with and without the hill on medium wet ( $\epsilon_{rs} = 15$ ;  $\sigma_s = 10^{-3} \text{ S} \cdot \text{m}^{-1}$ ) soil. The squared magnitude of the electric field is sampled at 9 km around the antenna and 1 m over the ground and normalized by the input power.

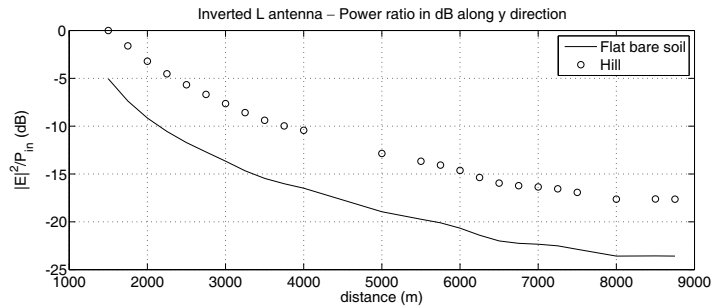


**Figure 12.** Simulations of an inverted L antenna at  $f = 100$  kHz with and without the hill on medium wet ( $\epsilon_{rs} = 15$ ;  $\sigma_s = 10^{-3} \text{ S} \cdot \text{m}^{-1}$ ) soil along  $y$  direction.

simulations, where the squared magnitude of the electric field is sampled at 9 km around the antenna and 1 m over the ground and normalized by the input power. On these figures one can note that the radiation pattern shapes do not change. Placing this antenna on a hill leads to a more efficient system for these two different soils.

Now the power ratio in dB is computed along  $y$  direction of propagation in Fig. 10 and Fig. 12. The values are sampled from 1.5 km to 9 km and 1 m over the soil far from the antenna and the end of the hill. One can see on these figures that the system is more efficient when it is located on the top of a hill, the gain of efficiency increasing with the wetness: 3 dB with on a dry soil and 6 dB on a medium wet soil.

### 3.2.2. Quarter-Wave Monopole Antenna

The inverted L antenna is replaced by a quarter-wave monopole antenna on a medium soil. The outputs shown in Fig. 13 and Fig. 14 are the same as the previous section. In all directions and on all distances of observation, the power ratio is upper of a few dB when the quarter-wave monopole antenna is built on the top of a hill, but of a much smaller amount.

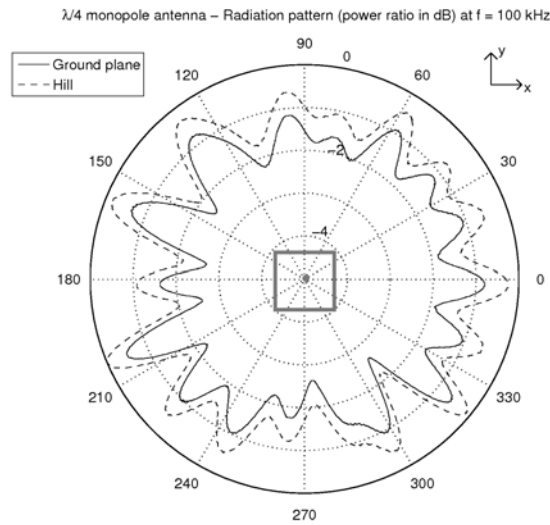


**Figure 13.** Simulations of a quarter-wave monopole antenna at  $f = 100$  kHz with and without the hill on medium wet ( $\epsilon_{rs} = 15$ ;  $\sigma_s = 10^{-3} \text{ S} \cdot \text{m}^{-1}$ ) soil. The squared magnitude of the electric field is sampled at 9 km around the antenna and 1 m over the ground and normalized by the input power.

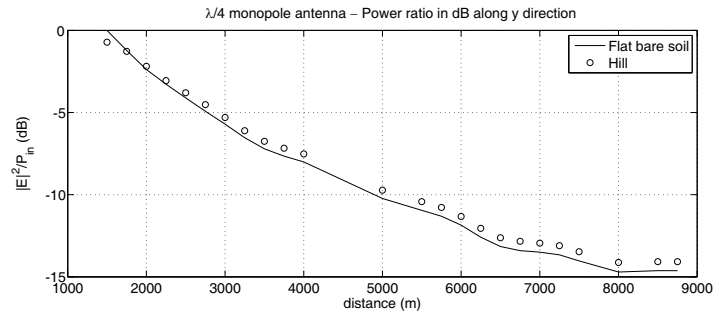


**Figure 14.** Simulations of a quarter-wave monopole antenna at  $f = 100$  kHz with and without the hill on medium wet ( $\epsilon_{rs} = 15$ ;  $\sigma_s = 10^{-3} \text{ S} \cdot \text{m}^{-1}$ ) soil along  $y$  direction.

## 4. CONCLUSIONS

To conclude on simulations of LF antennas with three-dimensional FDTD, results of infinitesimal dipole antenna computations are similar to two different methods and prove the efficiency of the PML boundaries: the near field is computed accurately up to a sufficient distance for this study. In this case, the subsequent use of the formula of DeMinco is an appropriate model to obtain the electric field values for long distance and curved Earth. By introducing a natural element close to an inverted L antenna, the shape of the radiation pattern is not affected, but a forest introduces losses whereas the system is more efficient when the antenna is located on the top of a hill. These effects are demonstrated in the figures of Section 3. On the other hand, the forest does not affect the radiation of a quarter-wave monopole antenna, whereas the hill favors it. One can deduce from these observations that the effects of a forest depend on the geometry of the antenna. On the contrary, the radiations of all antennas involved in this paper are more efficient when they are located on the top of a hill. A new strategy, using the 3D FDTD method and a numerical integration of Sommerfeld's problem, will be developed to extend in the far-field of low frequency antennas in the study of natural environments.

## REFERENCES

1. Rudge, A. W., K. Milne, A. D. Olver, and K. Knight, *The Handbook of Antenna Design Volumes 1 and 2*, Peter Peregrinus Ltd, London, 1986.
2. Maclean, T. S. M. and Z. Wu, *Radiowave Propagation Over Ground*, Chapman & Hall, London, 1993.
3. DeMinco, N., "Propagation prediction techniques and antenna modeling (150 to 1705 kHz) for intelligent transportation systems (ITS) broadcast applications," *IEEE Antennas and Propagation Magazine*, Vol. 42, No. 4, 9–34, August 2000.
4. Tsang, L., C.-C. Huang, and C. H., Chan, "Surface electric fields and impedance matrix elements of stratified media," *IEEE Transactions on Antennas and Propagation*, Vol. 48, No. 10, 1533–1543, October 2000.
5. Belrose, J. S., W. L. Hatton, C. A. McKerrow, and R. S. Thain, "The engineering of communication systems for low radio frequencies," *Proceeding of the IRE*, Vol. 47, No. 5, 661–680, May 1959.
6. Yee, K. S., "Numerical solution of initial boundary value problems involving Maxwell's equations in isotropic media," *IEEE Transactions on Antennas and Propagation*, Vol. 14, No. 3, 302–307, May 1966.
7. Taflove, A. and S. C. Hagness, *The Finite-Difference Time Domain Method*, Artech House, London, 2005.
8. Zhou, L., X. Xi, J. Liu, and N. Yu, "LF ground-wave propagation over irregular terrain," *IEEE Transactions on Antennas and Propagation*, Vol. 59, No. 4, 1254–1260, April 2011.
9. Holland, R. and L. Simpson, "Finite-difference analysis of EMP coupling to thin struts and wires," *IEEE Transactions on Electromagnetic Compatibility*, Vol. 23, No. 2, 88–97, May 1981.
10. Hubral, P. and M. Tygel, "Analysis of the Rayleigh pulse," *Geophysics*, Vol. 54, No. 5, 654–658, May 1989.
11. Von Hippel, A. R., *Dielectric Materials and Applications*, M.I.T. Press, Cambridge, 1954.
12. Berenger, J. P., "A Perfectly Matched Layer for the absorption of electromagnetic waves," *J. Computational Physics*, Vol. 114, 185–200, 1994.
13. Chew, W. C. and W. H. Weedon, "A 3D perfectly matched medium from modified Maxwell's equations with stretched coordinates," *IEEE Microwave Guided Wave Lett.*, Vol. 7, 599–604, 1994.
14. Roden, J. A. and S. D. Gedney, "Convolutional PML (CPML): An efficient FDTD implementation of the CFS-PML for arbitrary media," *Microwave Optical Tech. Lett.*, Vol. 27, 334–339, 2000.
15. De Moerloose, J. and M. A. Stuchly, "Behavior of Berenger's ABC for evanescent waves," *IEEE Microwave and Guided Wave Letters*, Vol. 5, No. 10, 344–346, October 1995.
16. Gedney, S. D., "An anisotropic Perfectly Matched Layer absorbing medium for the truncation of FDTD lattices," *IEEE Transactions on Antennas and Propagation*, Vol. 44, No. 12, 1630–1639, December 1996.
17. Sommerfeld, A., "Propagation of waves in wireless telegraphy," *Annalen der Physik*, Vol. 28, 665–736, March 1909.
18. Tewari, R. K., S. Swarup, and M. N. Roy, "Evaluation of relative permittivity and conductivity of forest slab from experimental measured data on lateral wave attenuation constant," *International Journal of Electronics*, Vol. 61, 597–605, November 1986.
19. Millington, G., "Ground-wave propagation over an inhomogeneous smooth Earth," *Proc. IRE*, Vol. 96, No. 39, 53–64, 1949.